Research Article Vol. 28, No. 11 / 25 May 2020 / Optics Express 16003
Optics EXPRESS

Coherent phonon dynamics in a c-plane sapphire crystal before and after intense femtosecond laser irradiation

XIN ZHAO,[1] ZHAOGANG NIE,[1,5] LIN MA,[1] FANGTENG ZHANG,[1] MINGMING HAO,[2,6] BO WANG,[1] WEIREN ZHAO,[1] LI LUO,[1] JIAHUA ZHANG,[3] AND CHUNG-CHE HUANG[4]

[1]*School of Physics and Optoelectronic Engineering, Guangdong University of Technology, Guangzhou 510006, Guangdong, China*
[2]*School of Materials and Energy, Guangdong University of Technology, Guangzhou 510006, China*
[3]*State Key Laboratory of Luminescence and Applications, Changchun Institute of Optics, Fine Mechanics and Physics, Chinese Academy of Sciences, Changchun, China*
[4]*Optoelectronics Research Centre, University of Southampton, Southampton SO17 183, UK*
[5]*zgnie@gdut.edu.cn*
[6]*haomm@gdut.edu.cn*

Abstract: Femtosecond pump-probe experiments with a ~6.4 fs time-resolution were performed to investigate the coherent phonon dynamics in a c-plane sapphire crystal before and after intense 800 nm femtosecond laser irradiation. The intense femtosecond laser induced defect/distortion and even re-crystallization of crystalline structures, which result in the appearance of new peaks and relative intensity change in coherent phonon and Raman spectra. The combination of these two spectra was found to be beneficial to evidence the variation of crystalline structure and further to differentiate the origins of new Raman peaks after irradiation. Further analysis of time-dependent differential absorbance with damped cosine function fitting and Fourier transfer calculation yields the vibrational parameters, including periods, damping times and initial phases, before and after irradiation. With these parameters, the defect-effects on damping time and the mechanism of coherent phonon generation were addressed.

1. Introduction

Sapphire has been intensively studied as substrate materials due to its excellent mechanical, physical and chemical properties [1–4], such as high transmittance, high hardness, high melting point, strong abrasion resistance and corrosion resistance, and so on. It has been widely used as optical window material in the field of aerospace and military affairs, where it is exposed to various harsh environments, for example, high-energy radiation, high-speed particles irradiation, etc. It was reported that exposure to high-energy radiation will induce the creation of crystal defects or distortion of the crystal lattice, leading to degradation of the service performance of the windows [5–7]. On the other hand, as excellent transparent materials, microscopic structure modifications via introduction of defects or voids achieved by tightly focusing a femtosecond (fs) laser on the surface or inside sapphire have been applied to fabricate various micro-optical components, such as micro-gratings and optical waveguides [8,9]. To study the structure and defect properties in sapphire is therefore closely related to the performance of sapphire windows and micro-optical devices. Due to the high transmittance of materials, conventional static absorption spectra are not suitable for the research. Raman spectroscopy has been used [10,11]. However, some fluorescence peaks of trace impurity ions are almost inevitably mixed in Raman spectroscopy, which makes it difficult to distinguish real Raman-active modes [11–13]. Ultrafast coherent phonon (CP) or coherent lattice vibration is quite sensitive to the structural evolution of

#392505 https://doi.org/10.1364/OE.392505
Journal © 2020 Received 11 Mar 2020; revised 5 May 2020; accepted 6 May 2020; published 13 May 2020

Optics EXPRESS

materials [14–17]. The study of CP dynamics in sapphire is consequently significant to reveal its structure and defect effects in extreme conditions.

Although the physical picture of laser-matter interaction is not completely clear, it is generally believed that photoionization is the basic mechanism for fs-laser utilized in material microprocessing, similar to the high-energy radiation [7,18,19]. In addition to being a defect/lattice distortion creator in transparent materials, fs-laser has also been shown over the past few decades to be a very effective tool to study coherent lattice oscillations (or CP) [20]. The defect-effects on CP dynamics have been investigated by femtosecond pump-probe and coherent anti-Stokes Raman spectroscopy (CARS) in various materials, such as bismuth films [21] and graphite [22], etc. However, only few reports on CP of sapphire. Xin Du et al. recently studied the CP dynamics in sapphire irradiated with 60Co γ-rays by fs-CARS technique with a 110 fs laser source [15]. They observed two quantum-beat signals with only a few cycles. Especially, the laser pulse duration in most of the work on ultrafast spectroscopy is hitherto around 100 fs or even longer. It is only suitable for the study of low-frequency vibrations since the CP generation requires the pulse duration much shorter than the phonon periods [14,19]. It was reported that typical Raman spectrum of sapphire crystal includes at least 7 active phonon modes ($2A_{1g} + 5E_g$) [10], thus further studies necessitate much shorter pulse duration to resolve more details of the CP dynamics. The ultra-short pulse duration of sub-10 fs laser is well-suited to achieve real-time observation of phonon dynamics with unprecedented high time resolution, and furthermore to allow an extension of the frequency scope studied to be more than 3000 cm^{-1} (equivalent to a vibrational period of ~10 fs).

In this work, CP dynamics in c-plane sapphire crystal before and after intense femtosecond laser irradiation was investigated by a ~6.4 fs time-resolved pump-probe experiment. Obvious oscillation signals due to coherent phonons were observed in transient absorption spectra. The intense fs-laser induced defect/distortion of crystalline structures, which brought about appearance of relative intensity change and even new peaks in CP and Raman spectra. The distinction of their origins was achieved by comparing the difference between CP and Raman spectra. Vibrational parameters, including periods, damping times and initial phases, were compared by performing damped cosine function fitting of the real-time traces before and after irradiation. The defect-effects on damping time and the mechanism of CP generation were further discussed.

2. Experimental section

The transparent c-plane sapphire of the order of centimeters in size, produced by Semiconductor Wafer, Inc. (SWI) is single crystal wafer with thickness of ~430 μm. The intense fs-laser (800 nm, 7 W, 1 kHz, 35 fs) is from a regenerative amplifier (Spectra-Physics, Solstice Ace). The laser beam was split into two parts. A part of it with pulse energy of 2 mJ was focused into the sample with radius of 150 μm (peak intensity = 8.08×10^{13} W/cm^2). The sample was irradiated for 2 hours. After irradiation, the sample is still transparent and no noticeable damage can be observed with eyes. Raman measurements with spectral resolution ≤ 0.35cm^{-1} were conducted on a Raman spectrometer LabRAM HR Evolution from HORIBA Jobin Yvon with excitation wavelength of 532.1 nm.

The other part of the laser pulse (800 nm, 5 W, 1 kHz, 35 fs) was used to construct the pump-probe system, as shown in Fig. 1(a). The pulse is firstly broadened by self-phase modulation through a hollow core fiber (HCF) filled with noble gas. The output white light beam are ~3.0 mJ@1 kHz with 480–1000 nm bandwidth (see Fig. 1(b), no noticeable sample absorption in the entire spectral range), which is subsequently compressed with a set of chirped mirrors. The compressed laser beam was used for optical pump-probe setup. The setup (see Fig. 1(a)) consists of a motorized translation stage, which is incorporated into the pump arm to generate a computer controlled time delay between pump and probe pulses. The pulse energies of pump and probe were adjusted by a combination of a half-wave plate and a polarizer. The transient absorption

Optics EXPRESS

signal was obtained by measuring the differential absorbance change $\Delta A = -\log_{10}(1+\Delta T/T)$, where $\Delta T/T = (T_{on}-T_{off})/T_{off}$, T_{on} and T_{off} are the intensity of the transmitted probe light passing through the sample in both the presence and absence of the pump excitation. The time resolution of the apparatus is ~6.4 fs, as determined by the ~9 fs FWHM (see inset of Fig. 1(b)) of the second-order intensity cross-correlation trace between pump and probe pulses. The time zero and instrument response in time-domain were determined to <1 fs accuracy by the cross-correlation measurement in a 10 μm thick BBO crystal located at the position of the sample target. During the experiment, the pump light was vertically polarized, while the probe light was horizontally polarized. Typical pulse energies for the pump and probe beams are 160 and 20 nJ, respectively. The pump and probe beams have focal spot diameters ($1/e^2$) of ~240 and 200 μm, respectively. Fluence dependence studies confirm that the ΔA signal is far from saturated because it remains linear to at least three times the pulse energies used in the experiments.

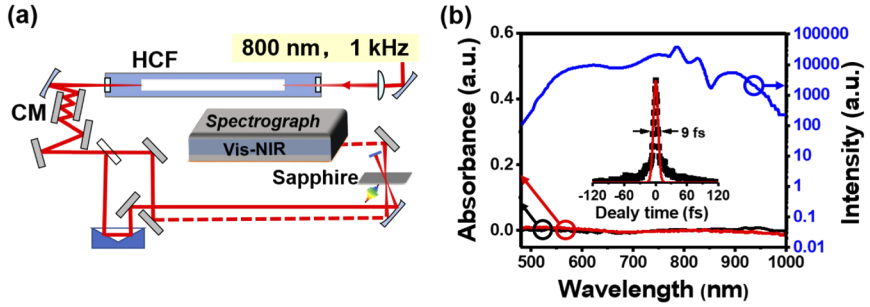

Fig. 1. (a) schematic diagram of the pump-probe setup. (b) Laser pulse (blue line) employed in pump-probe experiment, and absorption spectra of c-plane sapphire crystal before (black line) and after (red line) intense fs-laser irradiation. Inset: cross-correlation trace (black line) of the pump and probe pulses with its Gaussian fitting curve (red line). The FWHM of the autocorrelation trace is ~9 fs, corresponding to a time resolution of ~6.4 fs.

3. Results and discussion

Two-dimensional (2D) ΔA spectra before and after laser irradiations are plotted against probe wavelength and delay time in Figs. 2(a) and (b), respectively. For both of them, the obvious striped oscillatory structures perpendicular to the time axis represent the modulation of the difference absorbance δΔA. Here δ is the modulation of ΔA due to CPs, which give rise to the vertical signal modulations. Typical real-time traces are displayed later in Figs. 3(a) and (b). CP spectra before and after irradiation were obtained by performing Fourier transfer (FT) of ΔA spectra, as depicted in Figs. 2(c) and (d), respectively. The striped structures parallel to the horizontal axis are due to the distributions of CP intensity along probe wavelength. Except for the significant oscillations, there are no other transient signals, such as ground state bleach, stimulated emission and excited absorption, which are related to electronic transitions and usually appear in conventional ΔA spectra. According to displacive excitation theory [23], the CP can be generated either in the excited state via the simultaneous coherent excitation of vibronic polarizations or in the ground state via impulsive stimulated Raman scattering (ISRS). However, the situation is simpler for transparent sapphire [16,17], since there is no dipole allowed electronic transitions available in the pump and probe wavelength range. Thus no contribution from the transition probability change is expected in ΔA spectra. In this case, the pump induced polarization, $P^{(3)}(\omega,\tau)$, is generated by a Raman gain/loss process associated with energy exchange between the coherent vibrations and the probe optical field, according to the relation $\Delta A(\omega,\tau) \propto -\mathrm{Im}[P^{(3)}(\omega,\tau)/E_{probe}(\omega,\tau)]$ [14]. The probe optical field is alternately amplified and de-amplified, leading to the vibrational signals

Optics EXPRESS

in ΔA. Detailed mechanism of the CP generation will be addressed later by the initial phase analysis in Fig. 4. The intensity distribution of the oscillations along the probe wavelength is not homogeneous, since it could be affected by the laser intensity distribution and small chirp difference in different pump wavelength positions [14,20,24]. The exact mechanisms responsible for the CP amplitude profiles need to be further investigated.

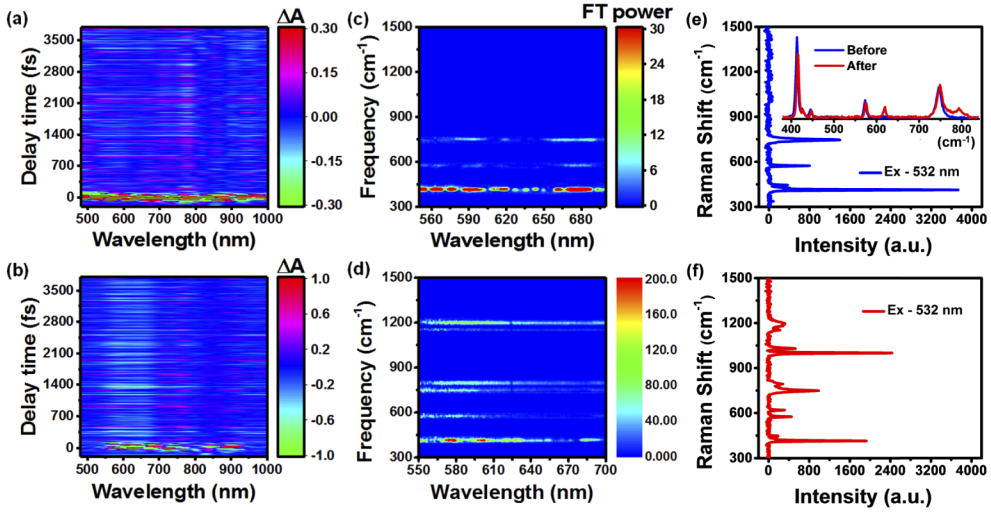

Fig. 2. 2D ΔA spectra probed as a function of time delay and probe wavelength before (a) and after (b) fs-laser irradiation with their corresponding FT power spectra before (c) and after (d) irradiation, respectively. The FT calculation was done in the range of 550–700 nm, where the signal to noise ratio is higher than other wavelength range. Raman spectra of the sapphire crystal before and after fs-laser irradiation are shown in (e) and (f), respectively.

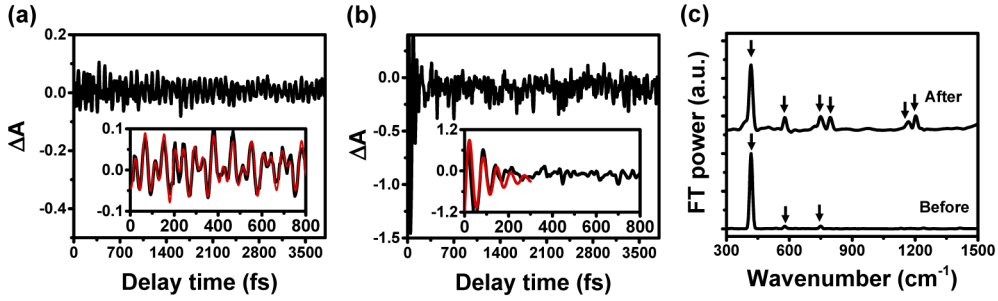

Fig. 3. Time traces detected from 0 to 3700 fs at the wavelength of 575 nm before (a) and after (b) irradiation, and their corresponding FT power spectra (c). The insets in (a) and (b) are the enlarged time traces in 20–800 fs range showing the pronounced vibrations. The data in the initial time range before 20 fs was deleted to avoid the influence of the coherent artifacts close to the zero time. The red line in the insets are the cosine fitting of the time traces.

The Raman shifts for different modes theoretically correspond to the vibrational frequencies in the FT spectra of their CPs. To assign the vibrational modes in the FT power spectra, Raman spectra of sapphire before and after fs-laser irradiation are compared in Figs. 2(e) and (f). Before irradiation, three conspicuous vibration modes at 413, 573 and 746 cm^{-1} were simultaneously detected by Raman and CP spectroscopies, indicative of phonon or Raman active origins of

Optics EXPRESS

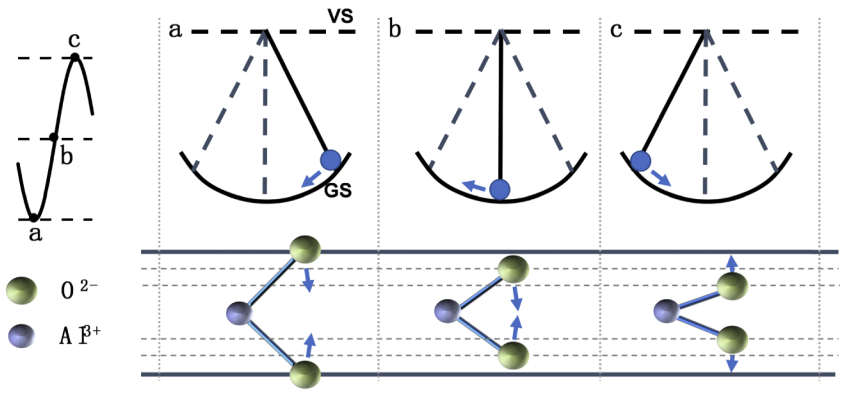

Fig. 4. Schematic of the relationship between the coherent phonon vibration and initial phase for the O-Al-O bending mode at 413 cm^{-1}. The three positions (a, b and c) on the oscillation waveform correspond to three moving positions of the "pendulum", which represents three moving positions of vibration packets on the ground state (GS) after "sudden" displacive excitation. The abbreviation VS stands for virtual state. The motion of the pendulum with different potential further represents different moving status of the O-Al-O bending mode.

these oscillations. The peak positions obtained by Gaussian fitting and their assignments of these bands (listed in Table 1, spectral resolution $\leq 0.35\,cm^{-1}$) are in good agreement with the experimental reports and theoretical predications based on group theory (D^6_{3d} symmetry) for α-Al_2O_3 [10]. After irradiation, in addition to the original peaks before irradiation, some new peaks emerge in the Raman and CP spectra with frequencies beyond $750\,cm^{-1}$, as compared later in Fig. 3. For the Raman spectrum, six new peaks are obtained in comparation with that before. Only three of them peaking at 793, 1152 and $1192\,cm^{-1}$ have equivalent peaks with the same frequencies in CP spectra. It is noted that there isn't detectable Raman modes beyond $900\,cm^{-1}$ before irradiation. Except for the emergence of new peaks, the relative intensity of the original peaks was obviously changed after irradiation. For example, the relative intensity between the peaks at $413\,cm^{-1}$ and $746\,cm^{-1}$ is ~0.69 times less than before. Moreover, tiny shifts in the Raman peak positions can be carefully discerned in the inset of Fig. 2(e), which displays the Raman spectra with frequencies below $850\,cm^{-1}$ before and after irradiation. The shift is consistent with the peak values listed in Table 1.

The appearance of new peaks and the detectable slight change of original peak positions are evident of distortion of crystalline structure or some new crystalline structure formed in the modified region by laser irradiation. A similar phenomenon characterized by Raman spectra has been observed in transparent quartz crystal in our group [25]. The distortion of crystalline structure could be due to defect formation, bond breaking, amorphization or material density variation. They slightly modified the lattice parameters, and manifested themselves in small Raman shifts. The new peaks, which have no equivalent phonon bands in FT power spectra, are probably due to fluorescence of transition metal ions, such as: Fe^{3+}, Ti^{3+}, Cr^{3+} and other trace elements, which are almost always present in alumina [10–13]. It was reported that trace amounts of Cr^{3+} and/or Fe^{3+} in aluminum oxide could induce strong fluorescence at special positions in Raman spectrum. Both re-crystallization and valence state manipulations of metal ions could occur. Free electrons and consequent avalanche ionization can be generated by multiphoton absorption at the laser focus, and as a consequence valence state manipulations along with re-crystallization could occur, leading to the fluorescence enhancement [7]. The early research with only Raman spectroscopy was limited by the difficulty in distinguishing real Raman-active modes from some fluorescence peaks of trace impurity ions [11]. The peaks at around 1152 and

Optics EXPRESS

Table 1. Assignments of peaks observed in the Raman spectra of sapphire before and after fs-laser irradiation.

Before irradiation Frequency (cm^{-1})	After irradiation Frequency (cm^{-1})	Assignments
413.35	415.67	A_{1g}
425.75	425.41	E_g
445.22	447.40	E_g
573.31	574.71	E_g
/	619.88	new fluorescence peak
745.79	749.08	E_g
/	793.13	New Raman peak
/	1001.18	new fluorescence peak
/	1029.31	new fluorescence peak
/	1152.32	new Raman peak
/	1192.93	new Raman peak

1192 cm^{-1} were previously attributed to the fluorescence of Fe^{3+} and/or Cr^{3+} in θ-Al_2O_3, and they appeared as evidence of the existence of θ-Al_2O_3 after re-crystallization in α-Al_2O_3 [11–13]. However, the concomitant appearance of corresponding FT peaks at the same frequencies reveals their partial phonon nature, which has not been detected before. Thus the combination of CP and Raman spectra is of great benefit for the verification of the origin of unknown peaks in Raman spectrum.

In order to evaluate the difference of vibrational parameters before and after irradiation in time domain, typical time trace probed at 575 nm were compared in Figs. 3(a) and (b). Their corresponding FT results are plotted in Fig. 3(c). For the traces before irradiation, there are three obvious vibrational modes peaking at 413 (mode 1), 573 (mode 2) and 746 cm^{-1} (mode 3) in the FT power spectra. Three new peaks at 794, 1159 and 1198 cm^{-1} are observed after irradiation, in good agreement with the 2D plot of FT spectra in Fig. 2. Note that the frequency reslution (> 2cm^{-1}) of the FT spectra is lower than that of the Raman spectra, so the peak positions obtained are slightly different from those in the Raman spectra. In order to avoid the influence from the coherent artifacts close to zero time, the FT calculation is performed on the data after 20 fs. The time trace can be accurately reproduced by a sum of three damped cosine functions related to the three CP modes with the following equation: $S(t) = \sum_i A_i e^{-t/\tau_i} \cos(2\pi w_i t + \varphi_i)$, where A_i, w_i, τ_i and φ_i (i = 1, 2, 3) are the initial amplitude, frequency, damping time and initial phase of the phonon oscillation, respectively. The vibrational parameters are summarized in Table 2. The obtained three periods ($T_i = 1/w_i$), 79.94, 57.67, and 44.46 fs, are respectively consistent with the frequencies (w_i) from FT calculation (see Fig. 3(c)) and Raman shift measurement (see Fig. 1(e)). The periods change little (not listed in Table 2) for irradiated sample, suggesting that the most lattice structure is only slightly modulated. Before irradiation, the damping times (τ_i) of the oscillations of 413.35 and 745.79 cm^{-1} are 5.37 and 0.96 ps, respectively. The latter one is consistent with the results in Xin Du's report for E_g phonon mode [15]. For the oscillation of 578 cm^{-1}, its damping time is longer than 10 ps, much longer than our pump-probe delay time (5 ps). After irradiation, more vibrations overlapped together in the time traces, making it difficult to fit the traces with a finite number of oscillations. However, inspection of the enlarged time traces shown in the inset of Fig. 3(b) suggests that the damping time for mode 1 is significantly shortened (< 1.0 ps). Damping times of other modes cannot be accurately obtained by cosine fitting. At different detection positions in the irradiated region, the damping times obtained may be different. But they are all more or less reduced (not shown). As discussed above, new

Optics EXPRESS

phonon modes, defects and fluorescence centers appear in irradiated samples, which may take effects as energy release channels. Thus the reduction is probably due to the acceleration of phonon-phonon scattering, which releases vibrational energy to the lattice and surroundings, or ascribed to electron-phonon scattering via defect states and fluorescent centers, which act as energy traps and thus enhance the damping effect.

Table 2. Summary of some vibrational parameters for three pronounced phonon modes before and after irradiations.[a]

	w_1 (cm^{-1})	w_2 (cm^{-1})	w_3 (cm^{-1})	τ_1 (ps)	τ_2 (ps)	τ_3 (ps)	φ_1 (π)	φ_2 (π)	φ_3 (π)
Before irradiation	413.35 (79.94 fs)	573.31 (57.67 fs)	745.79 (44.46 fs)	5.37 ± 1.5	>10	0.96 ±0.1	0.84 ± 0.01	0.94 ± 0.02	0.98 ± 0.01
After irradiation	414.77	574.71	748.86	< 1.0	-	-	0.78 ± 0.1	0.73 ± 0.01	0.25 ± 0.02

[a]The frequencies of the three modes are obtained by Gaussian fit of the corresponding Raman peaks in Figs. 2(e) and (f), respectively. The data below the frequencies in the brackets are the vibrational periods, obtained by cosine fitting of the time traces in Fig. 3(a). The initial phases are all from cosine fitting, except the phase 2 and phase 3 (φ_2 and φ_2), which are from FT calculations.

Analysis of the initial phases (φ_i) could provide insight into the mechanisms responsible for CP generation. The initial phases of the three modes before irradiation, obtained by cosine fitting of the typical time traces in Fig. 3, are also presented in Table 2. Before irradiation, all the phases are quite close to 0 or π, indicative of in-phase oscillation. Since many more vibrations mixed together than that before irradiation, only the phase 1 (φ_1) is estimated from cosine fitting, the other two phases are calculated from FT. All the phases are still close to 0 or π, but clearly they start moving to the $\pi/2$. Based on the theory of displacive excitation of CP, the most frequently cited theory currently, the ultrafast-laser pulse creates wave packet motion that couples to the vibrational modes, providing the force $F(t)$ to generate the CP [16]. As mentioned above, the wave packet motion can be on the ground and/or on the excited states, which make the initial phases behave as sine and/or cosine functions, corresponding to phases of $(\pi/2)$ (2m+1) and $m\pi$ respectively, where m is an integer [26]. However it is different for sapphire, since there is no dipole allowed electronic transitions available in the pump-probe spectral range. As an extension of the theory of transiently stimulated Raman scattering (TSRS) [16], virtual electronic excitations (as described by a Raman tensor) are included in the description of the force $F(t)$ for transparent materials. The key component of it is a Raman tensor that places both virtual and real electronic excitations on equal footing, thus making TSRS theory also applicable to transparent materials. In this case, the ground-state wave packet motion behaves as a cosine function with initial phase of $m\pi$.

To vividly describe the CP generation in sapphire, we take the O-Al-O bending mode at 413 cm^{-1} as an example. It can be easily understood by analogy to a simple "pendulum" which is subjected to an impulse driving force (see Fig. 4). This analogy is natural since the coherent lattice vibration behaves as a classical harmonic oscillator [27]. Through electrostriction (i.e., stimulated scattering), the electric field of the laser light exerts a classical $F(t)$ via the light-phonon coupling, which drives the oscillator in a particular direction. The force changes the equilibrium geometry and shifts the equilibrium from its original minimum potential energy position ω_i to a maximum with energy of ω_f, here $\omega_f - \omega_i = \pm\omega_p$ and ω_p is phonon frequency. Since the change of the equilibrium position is "sudden" compared to the response time of the nuclei, the pendulum (or oscillator) starts to "swing" periodically from its maximum position after the impulse. Thus, the contribution from the impulse is a step function-like perturbation, and produces a cosine-type oscillation with initial phase of $\pm\pi$. This sudden displacement impulsively excites the vibration modes, leading to ultrafast modulations of optical constants, such as refractive index, at ω_p, which naturally explains the oscillations in probe absorbance. The phase of the bending mode

Optics EXPRESS

tends to be close to π/2 after irradiation, probably due to some real electronic states of defects or impurity metal ions, which play roles in the phonon generation. As addressed above, with the involvement of real electronic states, the ground state phonon oscillation should behave as a sine function with initial phase of π/2 (2m+1) [26]. These two kinds of oscillations mix together, might result in the phase shift to π/2. However, the exact mechanism of the phase shift need to be further studied.

4. Conclusions

In conclusion, we investigated the CP dynamics in c-plane sapphire crystals before and after intense fs-laser irradiation by sub-10 fs pump-probe measurements. Obvious oscillation signals were observed in ΔA spectra. The intense irradiation induced defect/distortion and even re-crystallization of crystalline structures, leading to appearance of new peaks and relative intensity change in CP and Raman spectra. The combination of these two spectra is proved to be beneficial to differentiate the origins of new peaks, i.e., to distinguish whether they are from Raman active modes or fluorescent impurity ions. Vibrational parameters, such as periods, damping times and initial phases, were compared by performing damped cosine function fitting of the real-time ΔA traces before and after irradiation. The results indicate that the defect/distortion of crystalline structures cannot change the vibrational periods obviously. However, they could act as energy traps to enhance the damping effect, resulting in reduction of damping times. Furthermore, real electronic states of the defects and fluorescent centers may play roles in the ground state phonon vibrations, inducing obvious initial phase shift. Our study sheds new insights into the application of ultrafast CP spectroscopy to study of crystalline defect-effects induced by intense electromagnetic field.

Funding

National Natural Science Foundation of China (11704079, 11774071, 11874125); Guangzhou Municipal Science and Technology Project (201804010451, 201904010104); Guangdong University Students Science and Technology Innovation Training Special Foundation (pdjh2019b0155); State Key Laboratory of Luminescence and Applications (SKLA-2019-08); Guangdong Basic and Applied Basic Research Foundation (2019B1515120091); Research and Development Project in Key Area of Guangdong Province (2020B090922001).

Disclosures

The authors declare no conflicts of interest.

References

1. C. Ramesh, P. Tyagi, M. Senthil Kumar, M. and S, and S. Kushvaha, "Structural and Optical Properties of Self-Assembled Epitaxially Grown GaN Nanorods and Nanoporous Film on Sapphire (0001) Using Laser Molecular Beam Epitaxy," J. Nanosci. Nanotechnol. **20**(6), 3839–3844 (2020).
2. H. Liu and D. Chi, "Dispersive growth and laser-induced rippling of large-area singlelayer MoS_2 nanosheets by CVD on c-plane sapphire substrate," Sci. Rep. **5**(1), 11756 (2015).
3. G. Wang, M. Zhang, J. Han, X. He, H. Zuo, and X. Yang, "High-temperature infrared and dielectric properties of large sapphire crystal for seeker dome application," Cryst. Res. Technol. **43**(5), 531–536 (2008).
4. T. Vodenitcharova, L. C. Zhang, I. Zarudi, Y. Yin, H. Domyo, T. Ho, and M. Sato, "The effect of anisotropy on the deformation and fracture of sapphire wafers subjected to thermal shocks," J. Mater. Process. Technol. **194**(1-3), 52–62 (2007).
5. V. R. Farmer, "A review of reliability and quality assurance issues for space optics systems," Proc. SPIE **1761**, 14–24 (1993).
6. T. D. Henson and G. K. Torrington, "Space radiation testing of radiation resistant glass and crystals," Proc. SPIE **4452**, 54–65 (2001).
7. D. Tan, K. N. Sharafudeen, Y. Yue, and J. Qiu, "Femtosecond laser induced phenomena in transparent solid materials: Fundamentals and applications," Prog. Mater. Sci. **76**, 154–228 (2016).

Optics EXPRESS

8. J. Bai, G. Cheng, X. Long, Y. Wang, W. Zhao, G. Chen, R. Stoian, and R. Hui, "Polarization behavior of femtosecond laser written optical waveguides in Ti: Sapphire," Opt. Express **20**(14), 15035–15044 (2012).
9. D. Kim, W. Jang, T. Kim, A. Moon, K. S. Lim, M. Lee, I. B. Sohn, and S. Jeong, "Nanostructure and microripple formation on the surface of sapphire with femtosecond laser pulses," J. Appl. Phys. **111**(9), 093518 (2012).
10. M. Kadleíková, J. Breza, and M. Veselý, "Raman spectra of synthetic sapphire," Microelectron. J. **32**(12), 955–958 (2001).
11. A. Aminzadeh, "Excitation frequency dependence and fluorescence in the Raman spectra of Al_2O_3," Appl. Spectrosc. **51**(6), 817–819 (1997).
12. M. F. Luo, P. Fang, M. He, and Y. L. Xie, "Fluorescence spectroscopic study of the phase transformation of γ- Al_2O_3 at high temperatures," Phys. Status Solidi A **203**(8), 2065–2072 (2006).
13. J. Kákoš, P. Veis, and L. Pach, "Photoluminescence spectra and crystallization of θ- Al_2O_3 and α- Al_2O_3 from AlOOH-Fe $(NO_3)_3$ gels," J. Sol-Gel Sci. Technol. **21**(3), 167–172 (2001).
14. T. Kobayashi, Z. Nie, J. Du, K. Okamura, H. Kataura, Y. Sakakibara, and Y. Miyata, "Electronic relaxation and coherent phonon dynamics in semiconducting single-walled carbon nanotubes with several chiralities," Phys. Rev. B **88**(3), 035424 (2013).
15. D. Xin, Z. Mingfu, M. Qingkun, S. Yunfei, H. Xing, Y. Yanqiang, and H. Jiecai, "Phonon dynamics in γ-ray irradiated sapphire crystals studied by fs-CARS technique," Opt. Express **18**(22), 22937–22943 (2010).
16. D. M. Riffe and A. J. Sabbah, "Coherent excitation of the optic phonon in Si: Transiently stimulated Raman scattering with a finite-lifetime electronic excitation," Phys. Rev. B **76**(8), 085207 (2007).
17. F. Glerean, S. Marcantoni, G. Sparapassi, A. Blason, M. Esposito, F. Benatti, and D. Fausti, "Quantum model for impulsive stimulated Raman scattering," J. Phys. B: At., Mol. Opt. Phys. **52**(14), 145502 (2019).
18. S. Okazaki, "Comparison of Optical, X-ray, Electron and Ion Beam Lithography," Microelectron. Eng. **9**(1-4), 297–304 (1989).
19. T. Voisina, M. D. Grapes, Y. Zhang, N. Lorenzo, J. Ligda, B. Schuster, and T. P. Weihs, "TEM sample preparation by femtosecond laser machining and ion milling for high-rate TEM straining experiments," Ultramicroscopy **175**, 1–8 (2017).
20. T. Kobayashi, "Real-Time Spectroscopy of Molecular Vibrations with Sub-5-Fs Visible Pulses," *Femtosecond Laser Spectroscopy*, P. Hannaford, ed. (Springer, 2005), Chap.6, pp. 133–164.
21. M. Hase, K. Ishioka, M. Kitajima, K. Ushida, and S. Hishita, "Dephasing of coherent phonons by lattice defects in bismuth films," Appl. Phys. Lett. **76**(10), 1258–1260 (2000).
22. K. Ishioka, M. Hase, M. Kitajima, and K. Ushida, "Ultrafast carrier and phonon dynamics in ion-irradiated graphite," Appl. Phys. Lett. **78**(25), 3965–3967 (2001).
23. H. J. Zeiger, J. Vidal, T. K. Cheng, E. P. Ippen, G. Dresselhaus, and M. S. Dresselhaus, "Theory for displacive excitation of coherent phonons," Phys. Rev. B **45**(2), 768–778 (1992).
24. T. Kobayashi and Z. Wang, "Spectral Oscillation in Optical Frequency-Resolved Quantum-Beat Spectroscopy With a Few-Cycle Pulse," IEEE J. Quantum Electron. **44**(12), 1232–1241 (2008).
25. F. Zhang, Z. Nie, H. Huang, L. Ma, H. Tang, M. Hao, and J. Qiu, "Self-assembled three-dimensional periodic micro-nano structures in bulk quartz crystal induced by femtosecond laser pulses," Opt. Express **27**(5), 6442–6450 (2019).
26. M. Ikuta, Y. Yuasa, T. Kimura, H. Matsuda, and T. Kobayashi, "Phase analysis of vibrational wave packets in the ground and excited states in polydiacetylene," Phys. Rev. B **70**(21), 214301 (2004).
27. Y. X. Yan and E. B. Gamble Jr., "Impulsive stimulated scattering: General importance in femtosecond laser pulse interactions with matter, and spectroscopic applications," J. Chem. Phys. **83**(11), 5391–5399 (1985).